Absence of adipose differentiation related protein upregulates hepatic VLDL secretion, relieves hepatosteatosis, and improves whole body insulin resistance in leptin-deficient mice[S]

Benny Hung-Junn Chang, Lan Li, Pradip Saha, and Lawrence Chan[1]

Departments of Medicine and Molecular and Cellular Biology, Baylor College Of Medicine, Houston, TX 77030

Abstract **We previously showed that adipose differentiation related protein (*Adfp*)-deficient mice display a 60% reduction in hepatic triglyceride (TG) content. In this study, we investigated the role of ADFP in lipid and glucose homeostasis in a genetic obesity model, $Lep^{ob/ob}$ mice. We bred $Adfp^{-/-}$ mice with $Lep^{ob/ob}$ mice to create $Lep^{ob/ob}/Adfp^{-/-}$ and $Lep^{ob/ob}/Adfp^{+/+}$ mice and analyzed the hepatic lipids, lipid droplet (LD) morphology, LD protein composition and distribution, lipogenic gene expression, and VLDL secretion, as well as insulin sensitivity of the two groups of mice. Compared with $Lep^{ob/ob}/Adfp^{+/+}$ mice, $Lep^{ob/ob}/Adfp^{-/-}$ mice displayed an increased VLDL secretion rate, a 25% reduction in hepatic TG associated with improvement in fatty liver grossly and microscopically with a change of the size of LDs in a proportion of the hepatocytes and a redistribution of major LD-associated proteins from the cytoplasmic compartment to the LD surface. There was no detectable change in lipogenic gene expression. $Lep^{ob/ob}/Adfp^{-/-}$ mice also had improved glucose tolerance and insulin sensitivity in both liver and muscle. The alteration of LD size in the liver of $Lep^{ob/ob}/Adfp^{-/-}$ mice despite the relocation of other LDPs to the LD indicates a nonredundant role for ADFP in determining the size and distribution of hepatic LDs.**—Chang, B. H-J., L. Li, P. Saha, and L. Chan. **Absence of adipose differentiation related protein upregulates hepatic VLDL secretion, relieves hepatosteatosis, and improves whole body insulin resistance in leptin-deficient mice. *J. Lipid Res.* 2010.** 51: **2132–2142.**

Supplementary key words Adrp • lipid droplet • Tip47 • ob/ob • fatty liver

Nonalcoholic fatty liver disease (NAFLD) has reached epidemic proportions in the US (1) and is especially common in patients with obesity and type 2 diabetes. NAFLD is characterized by the accumulation of triglyceride (TG) and the appearance of lipid droplets (LDs) in hepatocytes. LDs encompass a neutral lipid core, mainly of TG and cholesteryl ester, enveloped by a phospholipid monolayer (2). Also on the surface are LD proteins (LDPs) that consist of a family of proteins called PAT-domain proteins (3–5; see below), along with other proteins with varied functions, such as lipid metabolic enzymes and proteins involved in vesicle trafficking (6–8). The presence of these specialized proteins suggests that LDs are not merely passive storage receptacles of cytosolic lipids but highly organized organelles involved in cellular metabolism (9–12).

The PAT-domain proteins, named after Perilipin (Plin1), adipose differentiation related protein (Adfp; Plin2), and Tip47 (Plin3), are the predominant LDPs. A new Plin-based nomenclature (as shown in parenthesis when it first appears in the text) for these LDPs was recently proposed (13), but we have followed the conventional nomenclature in this paper. Whereas perilipin expression is confined to adipose and steroidogenic tissues, *Adfp* and *Tip47* are present in multiple tissues. Perilipin-knock-out mice are almost completely devoid of body fat because of high basal lipolysis; they are resistant to diet-induced as well as genetic obesity, pinpointing the role of perilipins in the regulation of lipolysis (14, 15). *Adfp* ablation results in a marked reduction in hepatic TG (16), reduced cholesterol

This research is supported in part by a Public Health Service grant DK56338, which funds the Texas Gulf Coast Digestive Diseases Center, and by a National Institutes of Health Grant HL-51586 (to L.C.). Its contents are solely the responsibility of the authors and do not necessarily represent the official views of the National Institutes of Health or other granting agencies. This research is also supported by the Diabetes and Endocrinology Research Center (P30DK079638) at Baylor College of Medicine. L.C. was also supported by the Betty Rutherford Chair for Diabetes Research from St. Luke's Episcopal Hospital and Baylor College of Medicine and the T.T. & W.F. Chao Global Foundation.

Manuscript received 1 December 2009 and in revised form 27 April 2010.

Published, JLR Papers in Press, April 27, 2010
DOI 10.1194/jlr.M004515

Abbreviations: Adfp, adipose differentiation related protein; ITT, insulin tolerance test; LD, lipid droplet; LDP, lipid droplet protein; MTTP, microsomal triglyceride transfer protein; NALFD, nonalcoholic fatty liver disease; OGTT, oral glucose tolerance test; TG, triglyceride.

[1]To whom correspondence should be addressed.
e-mail: lchan@bcm.edu

[S] The online version of this article (available at http://www.jlr.org) contains supplementary data in the form of one table and seven figures.

ester storage and upregulated cholesterol efflux from macrophages (17), modestly lowered milk fat (18), and compromised retinyl ester transport and storage in the retina (19). The function of TIP47 and other newly described PAT family proteins, such as S3-12 (Plin4) (20) and LSDP5 (also known as MLDP, OXPAT, and Plin5) (21, 22), remains elusive.

The reduction of hepatic TG in Adfp-null mice presents us with an opportunity to study the role of *Adfp* in the development of NAFLD and its metabolic consequences. Lean C57Bl/6J mice, however, do not spontaneously develop NAFLD, so we decided to use the obese mouse model of NAFLD. *Leptin*-deficient ($Lep^{ob/ob}/Adfp^{+/+}$) mice are a model for NAFLD and type-2 diabetes. They are hyperphagic due to a mutation in the *Leptin* gene whose protein product is normally secreted from the adipose tissue to communicate with the brain as a satiety signal (23). Loss of functional *Leptin* causes $Lep^{ob/ob}/Adfp^{+/+}$ mice to become obese. Although *Leptin* also regulates other bodily functions (23), the severe obesity, hyperglycemia, hyperinsulinemia, and fatty liver development occur early in these mice. We hypothesized that absence of *Adfp* in the *Leptin*-deficient mice would reduce the hepatic TG and ameliorate hepatic fat accumulation and its metabolic consequences without altering their body weight and obesity. To test this hypothesis, we bred $Adfp^{-/-}$ mice into $Lep^{ob/ob}/Adfp^{+/+}$ mice to produce $Lep^{ob/ob}/Adfp^{-/-}$. We examined in these animals how the presence and absence of ADFP modulates cellular lipid homeostasis at the transcript, protein, and lipid substrate levels as well as the distribution/expression of other LDPs. Finally, we took advantage of this mouse model to study the relationship between fatty liver and insulin resistance (24, 25).

MATERIALS AND METHODS

Chemicals and reagents

All chemicals were purchased from Sigma Chemical, except lipid standards (Avanti Polar Lipid). Primary antibodies were purchased from Chemicon (GAPDH) and Progen (Guinea Pig anti-ADFP, GP40 mN1). Anti-ADFP, TIP47, and LSDP5 were generated through Strategic Diagnostics by immunizing rabbits with respective 6His-tagged, full-length recombinant proteins. Rabbit anti-ABHD5 was a gift from Dr. Takashi Osumi at University of Hyogo, Japan. Alexa 488-tagged anti-rabbit, anti-guinea pig, Alexa 555-tagged anti-rabbit, and anti-guinea pig antisera were obtained from Invitrogen. Mouse microsomal TG transfer protein (MTTP) antibody was generated previously (26).

Mice

$Adfp^{-/-}$ mice (16) were crossed to $Lep^{ob/ob}$ mice to generate $Lep^{ob/ob}/Adfp^{-/-}$ mice. $Lep^{ob/ob}/Adfp^{+/+}$ mice were used as controls. Mice were maintained in a temperature-controlled facility with 12 h light/dark cycles and free access to regular chow and water. Male mice of 8–12 weeks old were used throughout this study unless otherwise indicated, and all were in the C57BL/6J genetic background. All studies were conducted according to the "Principles of Laboratory Animal Care" (NIH publication No. 85023, revised 1985) and the guidelines of the IACUC of Baylor College of Medicine.

MRI

Whole body compositions of mice were analyzed by EchoMRI (Echo Medical Systems) according to the manufacturer's instructions.

Plasma chemistry analysis

We collected blood from the orbital plexus under isoflurane (Vedco) anesthesia. Plasma was frozen in aliquots at −20°C or used immediately after collection. We used enzymatic kits for determination of serum NEFA (Wako), glycerol (Sigma Aldrich), cholesterol, and TG (Infinity). Plasma glucose was monitored by glucometer and insulin was measured by ELISA (Mercodia).

Liver lipid analysis

We homogenized 200 mg liver tissues in 2 ml of PBS, extracted lipids from these homogenate according to Bligh and Dyer (27), and fractionated different lipid species by one dimensional TLC (silica Gel-60, Analtech), using petroleum ether/ether/glacial acetic acid (85:25:1). Lipids were visualized by incubating the TLC plate in saturated iodine chamber. For quantitative analysis of hepatic lipids, we followed the method of Schartz and Wolins (28) by first partitioning lipids from water-soluble components of the tissue extracts with organic extraction followed by colorimetric enzymatic detection kits for TG (Infinity), cholesterol, and cholesterol ester (BioVision).

Determination of rate of VLDL secretion in vivo

We quantified the rate of VLDL secretion in vivo by injecting intraperitoneally Pluronic F-127 (BASF Corporation; 2 mg/g body weight in PBS), a lipoprotein lipase inhibitor (29), and monitored the plasma TG before, and 1, 2, and 3 h afterwards using an enzymatic kit (Infinity).

Quantitative RT-PCR

We isolated RNA using an RNeasy mini-kit (Qiagen) and treated all samples (10 μg) with RNase-free DNase-I before using Superscript-II First Strand kit (Invitrogen) and oligo-dT primer to synthesize first strand cDNA (in 100 μL reaction volume). Two micoliters of these samples were used for quantitative PCR using iQ-SYBR Green Supermix (Bio Rad) under MX3000P system (Stratagene). Primer sequences used in this study are listed in supplementary Table I. We used geNorm algorithm (30) to determine the most stably expressed housekeeping reference genes as controls.

Western blot analysis

For Western blotting, equivalent amounts of protein homogenate were resolved by 4–15% SDS-PAGE, transferred to nylon membrane, and probed with specific antibodies for visualization by enhanced chemiluminescence (SuperSignal kit, Pierce). Semiquantitative protein analysis on Western blots was done using Image J Software.

Histology and immunohistochemistry

We removed a piece of liver and fixed it in formalin overnight before dehydration and paraffin embedding. Five micron sections were stained with hematoxylin and eosin or further processed for immunofluorescence staining by simultaneously labeling proteins with specific primary antibodies (listed in "Chemicals and Reagents") and subsequently labeled with fluorescence-tagged secondary antibodies as described previously (31). Images were analyzed under a Zeiss Axioplan-2 Imaging System.

Oral glucose tolerance test and insulin tolerance test

We performed oral glucose tolerance test (OGTT) and i.p. insulin tolerance test (ITT) on 12- to 14-week-old mice. For OGTT,

mice were gavaged with glucose (1.5 g/kg of body weight) after 4 h fasting. For ITT, fasted mice were injected (i.p.) with insulin (5 U/kg body weight, Humulin R; Eli Lily). Experiments were performed between 10 AM and 12 PM. Blood was taken before and 15, 30, 60, and 120 min after treatment for determination of glucose and insulin levels.

Hyperinsulinemic-euglycemic clamp

Hyperinsulinemic-euglycemic clamp was performed as described previously (32).

Isolation of LD fraction

We removed 200 mg of liver tissue, which was cut into tiny pieces, and soaked in 3.5 ml of cold 250-STMDPS (250 mM sucrose, 50 mM Tris-HCL, 5 mM $MgCl_2$, 1 mM DTT, 0.5 mM PMSF, and Spermidine 25μg/ml) buffer (33) in a nitrogen bomb (Parr Instrument). Tissue was homogenized and LD fraction isolated as described by Liu et al. (34). Briefly, total homogenate was centrifuged at 10,000 *g* for 10 min to remove debris. The supernatant was mixed well and an aliquot was saved for total liver protein analysis, and the rest was subjected to further ultracentrifugation at 45,000 *g* for 1 h to separate and recover LD fraction floated on the top, the aqueous cytosolic fraction in the middle, and the microsomal pellet at the bottom.

Statistical analysis

Student's *t*-test was used for statistical analysis. The Mann-Whitney test was used when sample size was small ($n < 5$). Differences were considered significant when $P < 0.05$.

RESULTS

Absence of ADFP does not affect the degree of obesity but attenuates the fasting hyperglycemia of *Lep*$^{ob/ob}$ mice

Lep$^{ob/ob}$/*Adfp*$^{-/-}$ mice had similar body weight and body composition by MRI as *Lep*$^{ob/ob}$/*Adfp*$^{+/+}$ mice (supplementary Fig. IA, B). They also had similar plasma lipids, liver transaminases (**Table 1**), and random nonfasting plasma glucose (Table 1); however, 4 h fasting plasma glucose was lower in *Lep*$^{ob/ob}$/*Adfp*$^{-/-}$ mice compared with *Lep*$^{ob/ob}$/*Adfp*$^{+/+}$ mice (Table 1).

Lep$^{ob/ob}$/*Adfp*$^{-/-}$ mice have reduced hepatosteatosis

Previously, we had shown that *Adfp*$^{-/-}$ mice displayed a 60% reduced hepatic TG content (40% of wild-type) (16). So we examined whether absence of ADFP also downregulates hepatic TG in *Lep*$^{ob/ob}$ mice. The gross appearance of the liver in *Lep*$^{ob/ob}$/*Adfp*$^{+/+}$ mice showed considerable pallor, consistent with fatty liver (**Fig. 1A**). The liver of the *Lep*$^{ob/ob}$/*Adfp*$^{-/-}$ mice, however, displayed a relatively normal reddish hue (Fig. 1A). There was no difference in liver weight. Essentially all hepatocytes of *Lep*$^{ob/ob}$/*Adfp*$^{+/+}$ mice were tightly packed with numerous moderate-sized LDs taking up the entire cytoplasmic space. In contrast, about one-half of the hepatocytes of *Lep*$^{ob/ob}$/*Adfp*$^{-/-}$ mice were notable for the presence of single (unilocular) or few (oligo-locular), huge-sized LDs with preservation of a small amount of cytoplasm (Fig. 1B). The *Lep*$^{ob/ob}$/*Adfp*$^{-/-}$ cells that did not contain these huge LDs contained far fewer LDs that were generally much smaller than those in hepatocytes of *Lep*$^{ob/ob}$/*Adfp*$^{+/+}$ mice.

We extracted total lipids from the liver and analyzed them by TLC, which showed that hepatic total TG was reduced in the *Lep*$^{ob/ob}$/*Adfp*$^{-/-}$ compared with the *Lep*$^{ob/ob}$/*Adfp*$^{+/+}$ mice. We used enzymatic kits to determine hepatic TG content, which was found to be reduced by ~25% in *Lep*$^{ob/ob}$/*Adfp*$^{-/-}$ (Fig. 1D). There was a ~50% increase in hepatic cholesterol in the *Lep*$^{ob/ob}$/*Adfp*$^{-/-}$ mice (Fig. 1D). Although cholesteryl ester was also increased in the *Lep*$^{ob/ob}$/*Adfp*$^{-/-}$ mice, the difference did not reach statistical significance.

TABLE 1. Body weight and plasma lipid and chemistry profiles of *Lep*$^{ob/ob}$/*Adfp*$^{+/+}$ and *Lep*$^{ob/ob}$/*Adfp*$^{-/-}$ mice (8–12 wk males, n = 6–10)

	Lep$^{ob/ob}$/*Adfp*$^{+/+}$	*Lep*$^{ob/ob}$/*Adfp*$^{-/-}$
Body weight (g)	48.3 ± 2.3	48.3 ± 3.4
TG (mg/dl)	40.7 ± 5.4	43.1 ± 10.7
Cholesterol (mg/dl)	139.3 ± 8.4	153.5 ± 28.3
Free fatty acids (mEq/L)	2.9 ± 0.4	3.1 ± 0.8
Glycerol (mg/dl)	47.5 ± 6.0	55.9 ± 2.7
ALT (U/L)	46.2 ± 20.4	27.6 ± 7.5
AST (U/L)	30.0 ± 6.6	27.6 ± 5.1
Glucose (fed; mg/dl)	159 ± 68	168 ± 75
Glucose (4 h fasted; mg/dl)	159 ± 42	131 ± 20*
Insulin (4 h fasted; μg/L)	12.8 ± 4.5	16.3±.3.8

* $P < 0.05$.

Lep$^{ob/ob}$/*Adfp*$^{-/-}$ liver displays increased VLDL secretion and MTTP expression

We measured VLDL secretion using the lipase inhibitor, Pluronic F-127 (29), and found a significantly increased rate of VLDL secretion in *Lep*$^{ob/ob}$/*Adfp*$^{-/-}$ compared with *Lep*$^{ob/ob}$/*Adfp*$^{+/+}$ mice (**Fig. 2A**). We next quantified the level of MTTP, the rate-limiting enzyme for VLDL assembly and secretion by Western blot analysis and found a markedly increased level of hepatic MTTP protein in *Lep*$^{ob/ob}$/*Adfp*$^{-/-}$ compared with *Lep*$^{ob/ob}$/*Adfp*$^{+/+}$ mice (Fig. 2B). To determine if the increased MTTP expression was also observed at the transcript level, we measured the relative level of MTTP mRNA by RT-PCR and found it to be the same in mice of the two genotypes (supplementary Fig. II), indicating that the MTTP protein overexpression in *Lep*$^{ob/ob}$/*Adfp*$^{-/-}$ mice occurred at a posttranscriptional level. By fast performance liquid chromatography analysis, we found that both HDL (cholesterol) and VLDL (TG) were increased in *Lep*$^{ob/ob}$/*Adfp*$^{-/-}$ mice compared with *Lep*$^{ob/ob}$/*Adfp*$^{+/+}$ mice (Fig. 2C, D), though total plasma TG and cholesterol were not different between the two groups (Table 1).

Lep$^{ob/ob}$/*Adfp*$^{-/-}$ mice display improved glucose tolerance compared with *Lep*$^{ob/ob}$/*Adfp*$^{+/+}$ mice

We examined the degree of glucose intolerance in these mice by oral GTT. In response to oral glucose, plasma glucose increased and peaked at 15 min in both *Lep*$^{ob/ob}$/*Adfp*$^{-/-}$ and *Lep*$^{ob/ob}$/*Adfp*$^{+/+}$ and tapered off in the next 2 h (**Fig. 3A**). During the test, the absolute glucose levels were significantly lower in every sampling point (except at 30 min) in *Lep*$^{ob/ob}$/*Adfp*$^{-/-}$ as compared with *Lep*$^{ob/ob}$/*Adfp*$^{+/+}$ mice (Fig. 3A). The corresponding insulin levels were not different between the two groups (Fig. 3B).

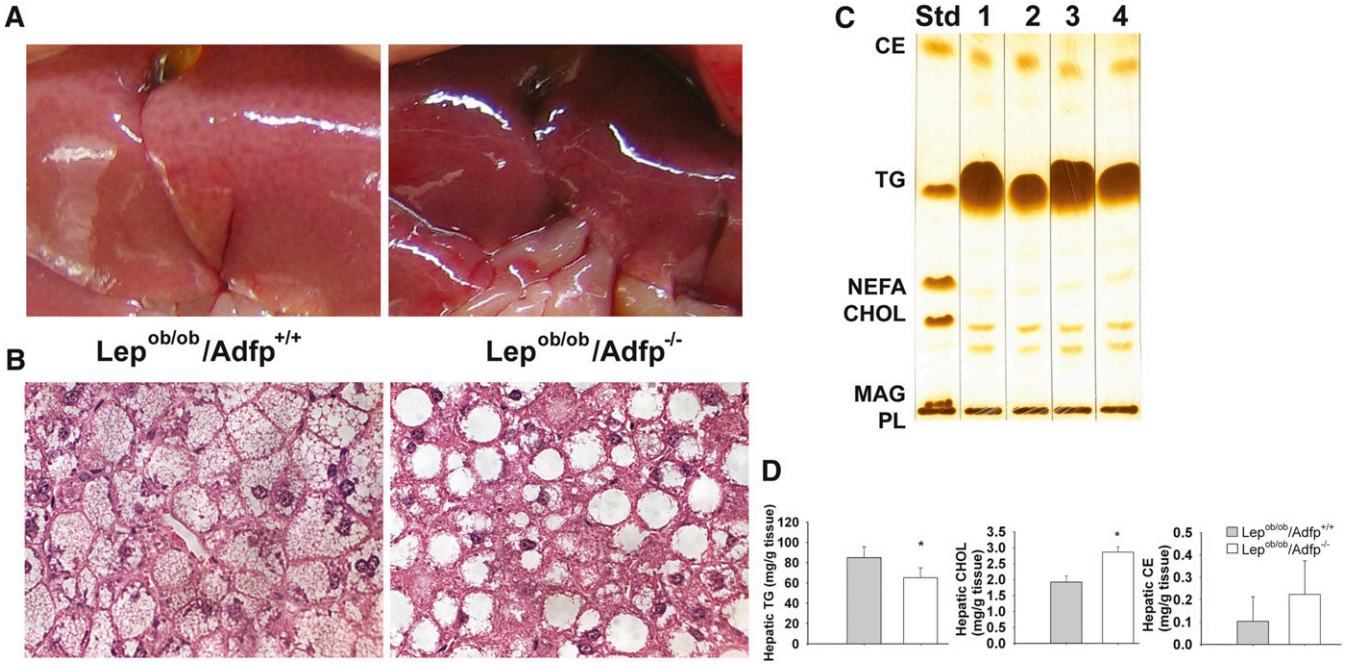

Fig. 1. Liver morphology, histology, and lipids in *Lep*$^{ob/ob}$*/Adfp*$^{+/+}$ and *Lep*$^{ob/ob}$*/Adfp*$^{-/-}$ mice. A: Liver morphology of one representative mouse. B: Hematoxylin and eosin staining of liver section; the white round areas are LDs. C: TLC analysis of hepatic lipids from representative *Lep*$^{ob/ob}$*/Adfp*$^{+/+}$ (lanes 1 and 3) and *Lep*$^{ob/ob}$*/Adfp*$^{-/-}$ (lanes 2 and 4) mice. Lipid standards (Std) used were cholesterol ester (CE), TG, cholesterol (CHOL), nonesterified fatty acid (NEFA), monoacylglycerol (MAG), and phospholipid (PL). D: Quantification of hepatic lipids determined by enzymatic methods (n = 4). $*P < 0.05$.

Lep$^{ob/ob}$*/Adfp*$^{-/-}$ and *Lep*$^{ob/ob}$*/Adfp*$^{+/+}$ mice display a similar glucose response during ITT

We performed an ITT as an initial test of insulin sensitivity. As shown in Fig. 3C, *Lep*$^{ob/ob}$*/Adfp*$^{+/+}$ mice responded to the insulin injection with a steeper drop in plasma glucose than the *Lep*$^{ob/ob}$*/Adfp*$^{-/-}$ mice (Fig. 3C), though there was no difference between the two groups when we expressed the results as percent drop in plasma glucose (Fig. 3D).

Hyperinsulinemic-euglycemic clamp reveals improved insulin action in *Lep*$^{ob/ob}$*/Adfp*$^{-/-}$ mice

As a more definitive test of insulin sensitivity in vivo, we performed a hyperinsulinemic-euglycemic clamp on the mice. Basal hepatic glucose production rate was similar in *Lep*$^{ob/ob}$*/Adfp*$^{-/-}$ and *Lep*$^{ob/ob}$*/Adfp*$^{+/+}$ mice (**Fig. 4A**). During the clamp, the *Lep*$^{ob/ob}$*/Adfp*$^{-/-}$ mice required a much higher glucose infusion rate to maintain euglycemia (Fig. 4B), indicating enhanced insulin sensitivity. They also exhibited an increased glucose disposal rate (Fig. 4C) compared with *Lep*$^{ob/ob}$*/Adfp*$^{+/+}$ mice, indicating a higher rate of peripheral glucose uptake in the *Lep*$^{ob/ob}$*/Adfp*$^{-/-}$ mice in response to insulin infusion, which also resulted in a better suppression of hepatic glucose production in *Lep*$^{ob/ob}$*/Adfp*$^{-/-}$ compared with *Lep*$^{ob/ob}$*/Adfp*$^{+/+}$ mice (Fig. 4D).

Gene transcript levels of metabolic enzymes

To determine if the reduced hepatic TG in *Lep*$^{ob/ob}$*/Adfp*$^{-/-}$ mice was a result of changes in gene expression involved in carbohydrate or lipid metabolic pathways, we isolated RNA from the liver of these mice and performed quantitative RT-PCR analysis. We examined the following genes involved in lipogenesis (Srebp-1c, Acc1, Fasn, and Scd-1), β-oxidation (Ppar-a, Cpt-1a, and Acadl), lipid transport (Ldlr and Mttp), and gluconeogenesis (G-6-Pase and Pepck) and found no difference in the expression level of any of these gene transcripts between *Lep*$^{ob/ob}$*/Adfp*$^{-/-}$ and *Lep*$^{ob/ob}$*/Adfp*$^{+/+}$ mice (supplementary Fig. II).

Altered abundance of LD-associated proteins in different cellular compartments but no change in their mRNA levels in the absence of ADFP

We previously showed that Adfp deficiency in vivo does not elicit a compensatory upregulation of other LDPs in primary mouse fibroblasts (16). However, we found in clonal cells derived from embryonic fibroblasts upregulated Tip47 gene expression in *Adfp*$^{-/-}$ cells upon lipid loading (35). Therefore, we examined whether LDPs and their transcripts were altered in the liver of the *Lep*$^{ob/ob}$*/Adfp*$^{-/-}$ mice. As many of the LDPs are localized both in the cytosol and LD, we determined by Western blotting the relative abundance of these proteins in total, cytosolic, and isolated LD fractions. PLIN, CIDE-A, -B and -C, ATGL, ADFP, TIP47, LSDP5, and ABHD5 were examined; however, only the last four were detectable in the liver by Western blotting (**Fig. 5**). These blots allowed us to compare the relative protein abundance in *Lep*$^{ob/ob}$*/Adfp*$^{-/-}$ and *Lep*$^{ob/ob}$*/Adfp*$^{+/+}$ liver from a particular subcellular fraction. We note that it would be inappropriate to compare the protein bands across different blots, because different antibodies and exposure times were used and protein recovery in individual fractions was not identical.

In the total protein extracts, we did not find any difference in the band intensity in TIP47. However, LSDP5 and ABHD5 were more abundant in the liver of *Lep*$^{ob/ob}$*/Adfp*$^{-/-}$

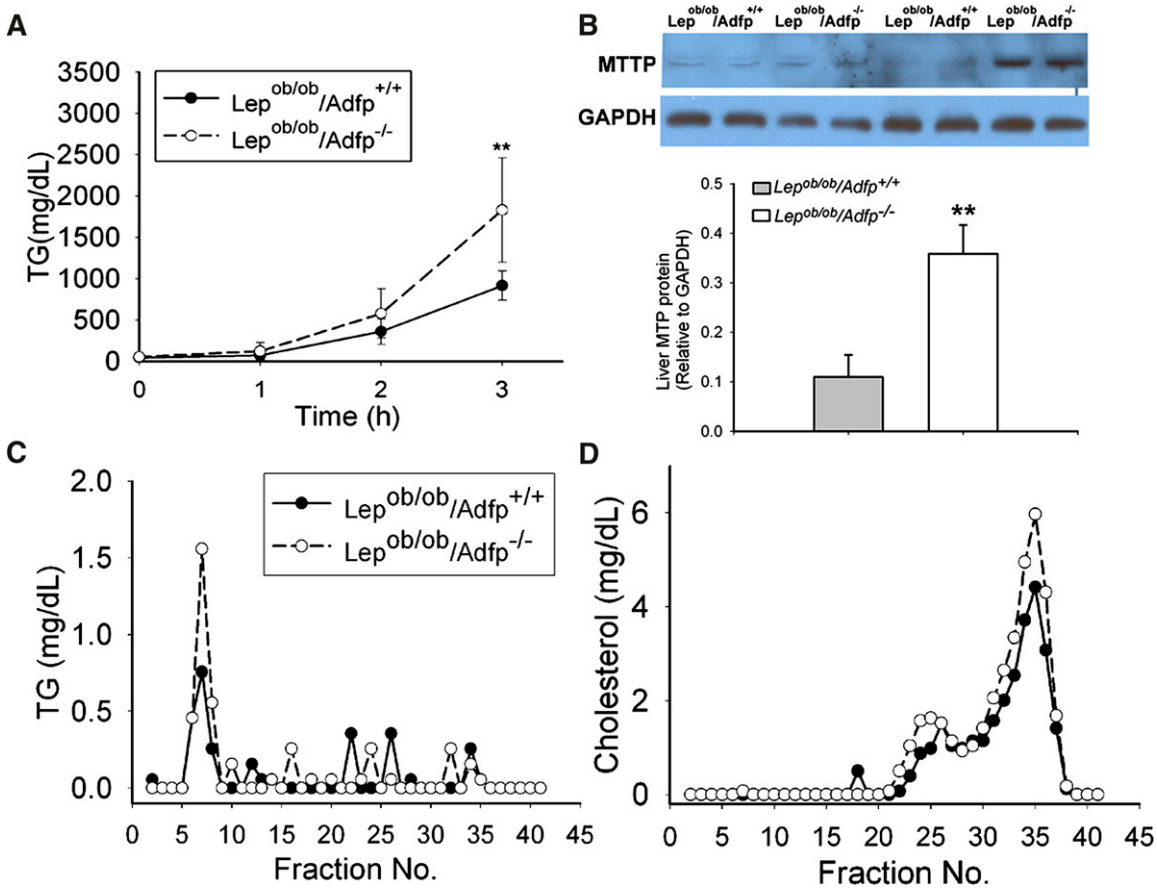

Fig. 2. Lipoprotein profiling of *Lep*$^{ob/ob}$/*Adfp*$^{+/+}$ and *Lep*$^{ob/ob}$/*Adfp*$^{-/-}$ mice. A: Rate of VLDL secretion in vivo (n = 6) measuring plasma TG before (0 h) and 1, 2, and 3 h after mice (fasted for 4 h) were treated with Pluronic F-127. B: Western blot analysis of hepatic MTTP. GAPDH was used as loading control. MTTP protein quantity (relative to GAPDH) was determined by densitometry of the Western blot (top panel) using Image J Software. $^{**}P < 0.01$. C and D: Plasma lipoprotein (pooled from three mice) analysis by fast performance liquid chromatography. The major TG peak between fractions 5 and 10 (in C) corresponds to the VLDL particles. The first cholesterol peak between fractions 20 and 30 represents IDL and LDL particles, and the second cholesterol peak between fractions 30 and 40 represents the HDL particles.

mice than *Lep*$^{ob/ob}$/*Adfp*$^{+/+}$ mice (Fig. 5A). Densitometric quantification revealed a more than 30-fold increase of LSDP5 in the *Lep*$^{ob/ob}$/*Adfp*$^{-/-}$ mice compared with *Lep*$^{ob/ob}$/*Adfp*$^{+/+}$ mice, using GAPDH as a loading control (Fig. 5A, bottom panel). ABHD5 was moderately (2-fold) increased in the liver of *Lep*$^{ob/ob}$/*Adfp*$^{-/-}$ mice compared with that of *Lep*$^{ob/ob}$/*Adfp*$^{+/+}$ mice. In the cytosolic fraction (after LD fraction was removed), we observed a small but significant increase in both LSDP5 and ABHD5 in *Lep*$^{ob/ob}$/*Adfp*$^{-/-}$ compared with *Lep*$^{ob/ob}$/*Adfp*$^{+/+}$ mice (Fig. 5B). The absence of ADFP in these blots confirmed the genotype of these samples.

We isolated LD fractions from the same liver samples and reconstituted the samples directly into protein gel loading buffer, because conventional aqueous buffer would not dissolve the hydrophobic proteins that co-purified with the lipids. Among the four proteins, we found an abundant amount of ADFP in *Lep*$^{ob/ob}$/*Adfp*$^{+/+}$ liver extracts, which was absent in *Lep*$^{ob/ob}$/*Adfp*$^{-/-}$ liver extracts (Fig. 5C). The amount of TIP47 in the LD fraction was significantly upregulated in *Lep*$^{ob/ob}$/*Adfp*$^{-/-}$ compared with *Lep*$^{ob/ob}$/*Adfp*$^{+/+}$ liver (Fig. 5C). Similarly, we found that LSDP5 and ABHD5 were also much more abundant in the LD fraction of *Lep*$^{ob/ob}$/*Adfp*$^{-/-}$ than *Lep*$^{ob/ob}$/*Adfp*$^{+/+}$ liver (Fig. 5C). GAPDH was not present in the LD fraction (Fig. 5C).

To determine if the change in protein abundance was the result of a change in mRNA expression, we measured the hepatic mRNA level of Tip47, Lsdp5, and Abhd5 genes by quantitative RT-PCR and found that the mRNA level for each of these proteins was similar between *Lep*$^{ob/ob}$/*Adfp*$^{-/-}$ and *Lep*$^{ob/ob}$/*Adfp*$^{+/+}$ mice (Fig. 5D).

LDs in *Lep*$^{ob/ob}$/*Adfp*$^{-/-}$ hepatocytes are enriched in TIP47

To further explore the difference in protein expression in some of the LDPs detected by Western blotting (Fig. 5), we performed immunofluorescence microscopy to determine the physical localization of ADFP, TIP47, LSDP5, and ABHD5 proteins in liver sections of *Lep*$^{ob/ob}$/*Adfp*$^{-/-}$ and *Lep*$^{ob/ob}$/*Adfp*$^{+/+}$ mice. Unfortunately, in our hands, the antibodies against LSDP5 and ABHD5 did not work for immunofluorescence staining, and we had to confine the immuno-morphological analysis to TIP47.

We simultaneously labeled ADFP and TIP47 with Alexa488 and Alexa555 fluorophores, respectively. In *Lep*$^{ob/ob}$/*Adfp*$^{+/+}$ hepatocytes, Alexa488-labeled ADFP decorated the small LDs, while TIP47 (Alexa555 labeled) was barely detectable

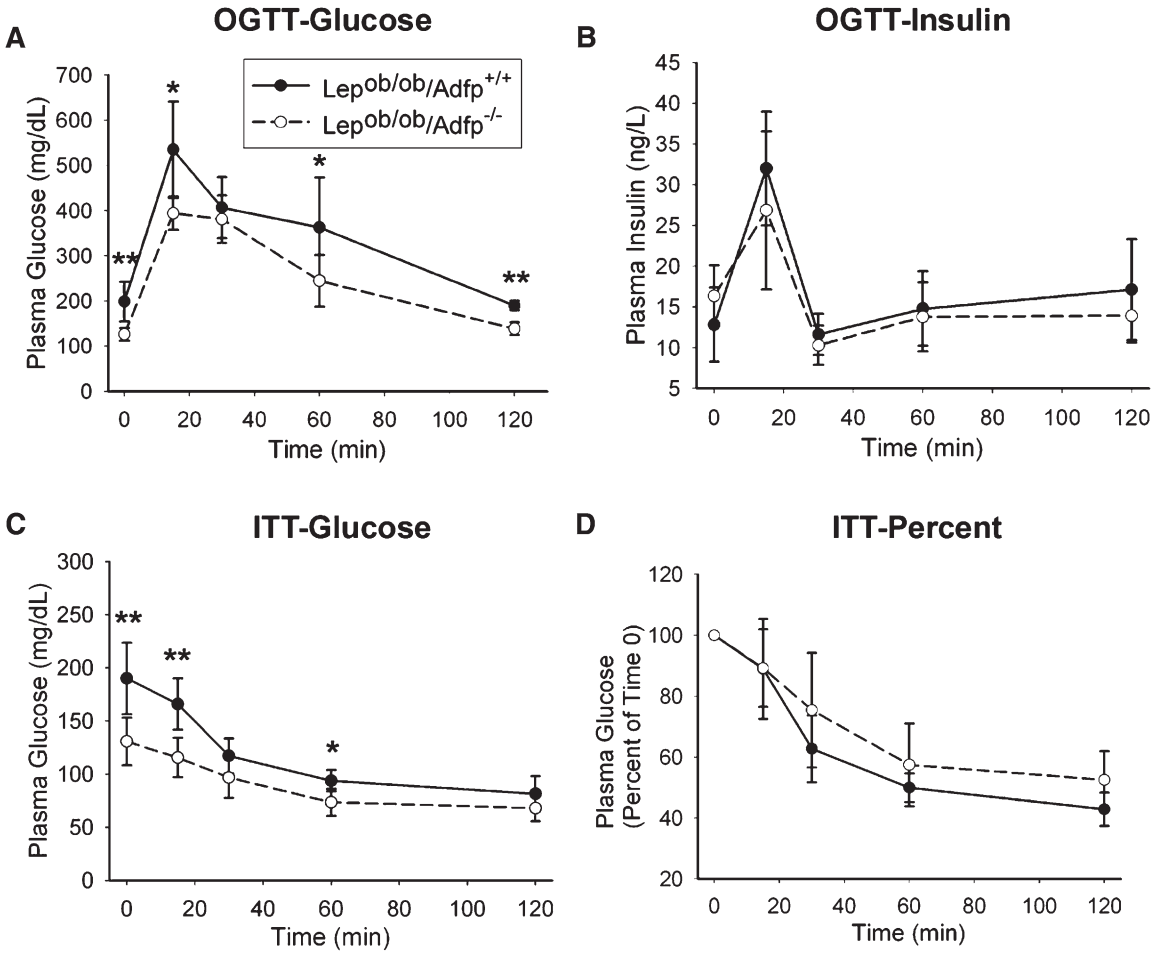

Fig. 3. OGTT and ITT in $Lep^{ob/ob}/Adfp^{+/+}$ and $Lep^{ob/ob}/Adfp^{-/-}$ mice (n = 6). A: Plasma glucose before and 15, 30, 60, and 120 min after glucose feeding (1.5 g/kg body weight); the corresponding plasma insulin level at each time point is shown in B. C: plasma glucose before and 15, 30, 60, and 120 min after i.p. insulin injection (5U/kg body weight). Percent value to glucose level at time 0 is shown in D. $*P < 0.05$; $**P < 0.01$.

and diffusely distributed in the cytoplasm (**Fig. 6**, top panels). In contrast, in $Lep^{ob/ob}/Adfp^{-/-}$ hepatocytes, ADFP was not detectable (because of the *Adfp* gene knock-out), while Alexa555-labeled TIP47 protein prominently lined the surface of LDs, in both large unilocular and smaller LDs (Fig. 6, bottom panels). This physical appearance is consistent with the results obtained from Western blot analysis.

DISCUSSION

By breeding $Adfp^{-/-}$ into $Lep^{ob/ob}$ mice, we produced a mouse model that exhibits attenuated hepatosteatosis in the presence of severe obesity compared with $Lep^{ob/ob}/Adfp^{+/+}$ mice. This improvement in fatty liver was associated with substantial changes in LD size and LDP distribution. The loss of ADFP also modulated the concentration and distribution of select LDPs, while it improved glucose tolerance and insulin insensitivity that plague $Lep^{ob/ob}$ mice.

We previously reported that *Adfp* deficiency in wild-type (lean) mice had an ~60% TG reduction in the liver in the absence of detectable changes in lipogenesis, lipid uptake, utilization, or transport (16). Importantly, we detected in these mice an increase in liver MTTP protein without any changes in mRNA expression. However, using Triton WR1339 to inhibit the vascular lipases, we previously found that the rate of VLDL secretion from the liver of $Adfp^{-/-}$ mice was similar to that of $Adfp^{+/+}$ mice. Recently, another lipase inhibitor called Pluronic F-127, also known as poloxamer 407, was reported to be less toxic and a better lipase inhibitor than Triton WR1339 for quantifying VLDL secretion in rodents in vivo (29). We therefore repeated the measurement using this new reagent and found that, indeed, $Adfp^{-/-}$ mice on a wild-type C57BL/6J background have a VLDL secretion rate significantly higher than that in $Adfp^{+/+}$ mice (supplementary Fig. III) despite $Adfp^{-/-}$ mice having a markedly reduced cytosolic TG content. Thus, we conclude that unbridled VLDL oversecretion occurs in $Adfp^{-/-}$ mice (in C57BL/6J genetic background), contributing to TG depletion in the liver.

We found in this investigation that, like wild-type mice, absence of ADFP in $Lep^{ob/ob}$ mice leads to increased hepatic MTTP expression at the protein but not mRNA level, as well as reduced TG content. We reasoned that a similar

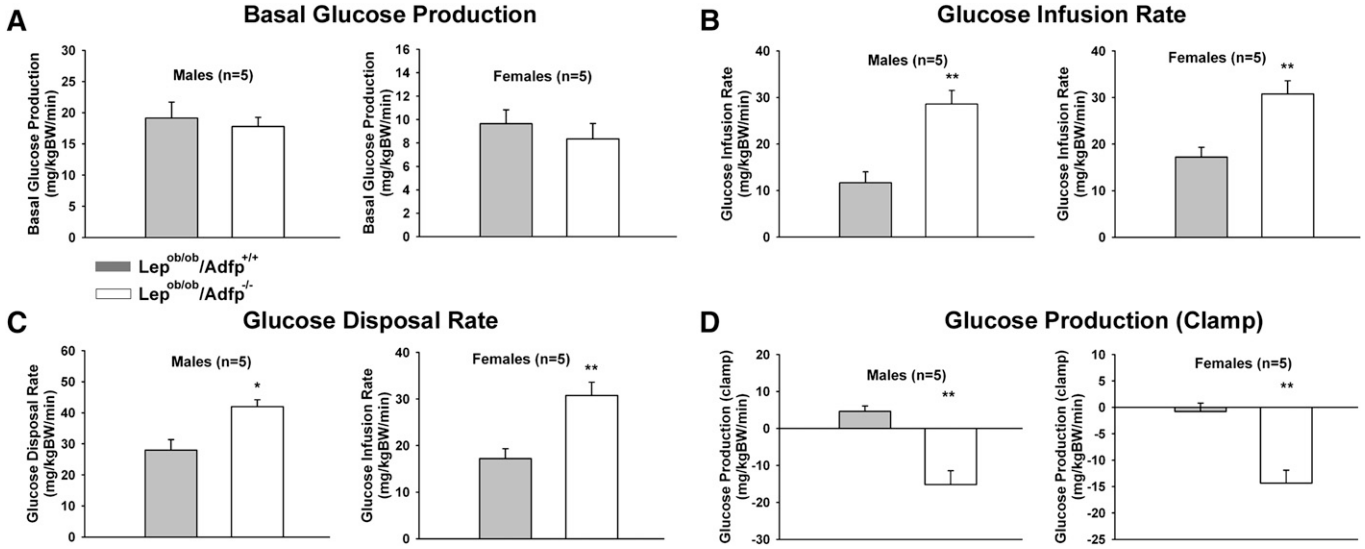

Fig. 4. Hyperinsulinemic-euglycemic clamp study of $Lep^{ob/ob}/Adfp^{+/+}$ and $Lep^{ob/ob}/Adfp^{-/-}$ mice (n = 5). A: Basal glucose production before insulin infusion. B: Rate of glucose disposal after clamp. Glucose infusion rate (C) and glucose production rate (D) after clamp.

mechanism likely underlies the improvement in the hepatosteatosis in these animals, a hypothesis that was confirmed by direct measurement of VLDL secretion using Pluronic F-127 (Fig. 2). We think that this is a key finding that underscores the important function of ADFP in lipid economy and homeostasis in the liver.

In addition to the decreased hepatic TG, we also found that the hepatic cholesterol was increased in the liver of $Lep^{ob/ob}/Adfp^{-/-}$ compared with that of the $Lep^{ob/ob}/Adfp^{+/+}$ mice. The amount of cholesterol in the liver was, however, much smaller compared with that of TG. The significance of the increased cholesterol in the $Lep^{ob/ob}/Adfp^{-/-}$ mice is unclear.

There is evidence that tissues other than the liver also display little redundancy in Adfp function as a key protein for efficient LD formation. We have demonstrated that macrophages export cholesterol more readily in Adfp deficiency, making them more resistant to foam cell formation. Furthermore, apolipoprotein E-deficient mice with ADFP deficiency are more resistant than ADFP-replete apolipoprotein E-deficient animals to atherosclerosis development, presumably because of the impaired foam cell formation in these animals (17). In our two previous studies (16, 17) and in the current investigation, we did not find any difference in lipid-related metabolic gene expression in tissues that are lipid-depleted because of ADFP deficiency. In addition to TG and cholesterol homeostasis, Imanishi et al. (19) showed that Adfp deficiency also caused abnormalities in retinyl ester homeostasis in the retinal pigmented epithelium, leading to delayed clearances of all-*trans*-retinal and all-*trans*-retinol from rod photoreceptor cells and resulting in impaired dark adaptation in the eye.

With respect to mammary gland function, Adfp-deficient mice coped well without ADFP in milk fat storage and secretion. An N-terminal truncated ADFP protein and its mRNA were found in the mammary gland (18), as well as retinal pigmented epithelium (19) of wild-type and *Adfp*-deficient (deletion of exons 2 and 3) mice. This N-terminal truncated ADFP protein seemed to be able to substitute for the function of the dominant form of ADFP in the mammary gland (18), but not in the retina function (19), perhaps due to an extremely low level of expression in the latter tissue. The N-terminal truncated form of ADFP was not sensitive to proteasome degradation as the full-length ADFP was (36). It also did not prevent TIP47 from accessing to the LD surface. In agreement with the previous study (18), using a combination of Western, Northern, and RT-PCR analyses, we did not detect the expression of the N-terminal truncated ADFP protein or mRNA in the liver of wild-type or knock-out mice (supplementary Fig. IV). The short truncated form seems to be specific to the mammary gland, and RT-PCR data suggests that an alternative transcription initiation site may reside in exon 4 (supplementary Fig. IVC).

Using an Adfp antisense oligonucleotide, Imai et al. (37) knocked down ADFP expression in the liver of $Lep^{ob/ob}$ mice and observed lowering of hepatic TG in treated mice. However, the mechanism seemed to be quite different from that in the knock-out model, because they observed significantly downregulated lipogenic gene expression in the liver of treated mice, contrary to our results in $Adfp^{-/-}$ mice with wild-type or $Lep^{ob/ob}$ background. In addition, they also observed a downregulation of VLDL secretion (37) instead of the upregulation that we found in both wild-type and $Lep^{ob/ob}$ mice that lack ADFP (supplementary Fig. III; Fig. 2A).

Hepatosteatosis is commonly associated with insulin resistance (38, 39). It has been suggested that obesity leads to chronic inflammation in adipose tissue, which releases pro-inflammatory cytokines that trigger insulin resistance that may somehow contribute to hepatosteatosis (40). Adfp deficiency in either wild-type (16) or $Lep^{ob/ob}$ background (current study) is not associated with a change in adipose or lean body mass (supplementary Fig. IB). It does not alter adipocyte differentiation or lipolysis in vitro or in

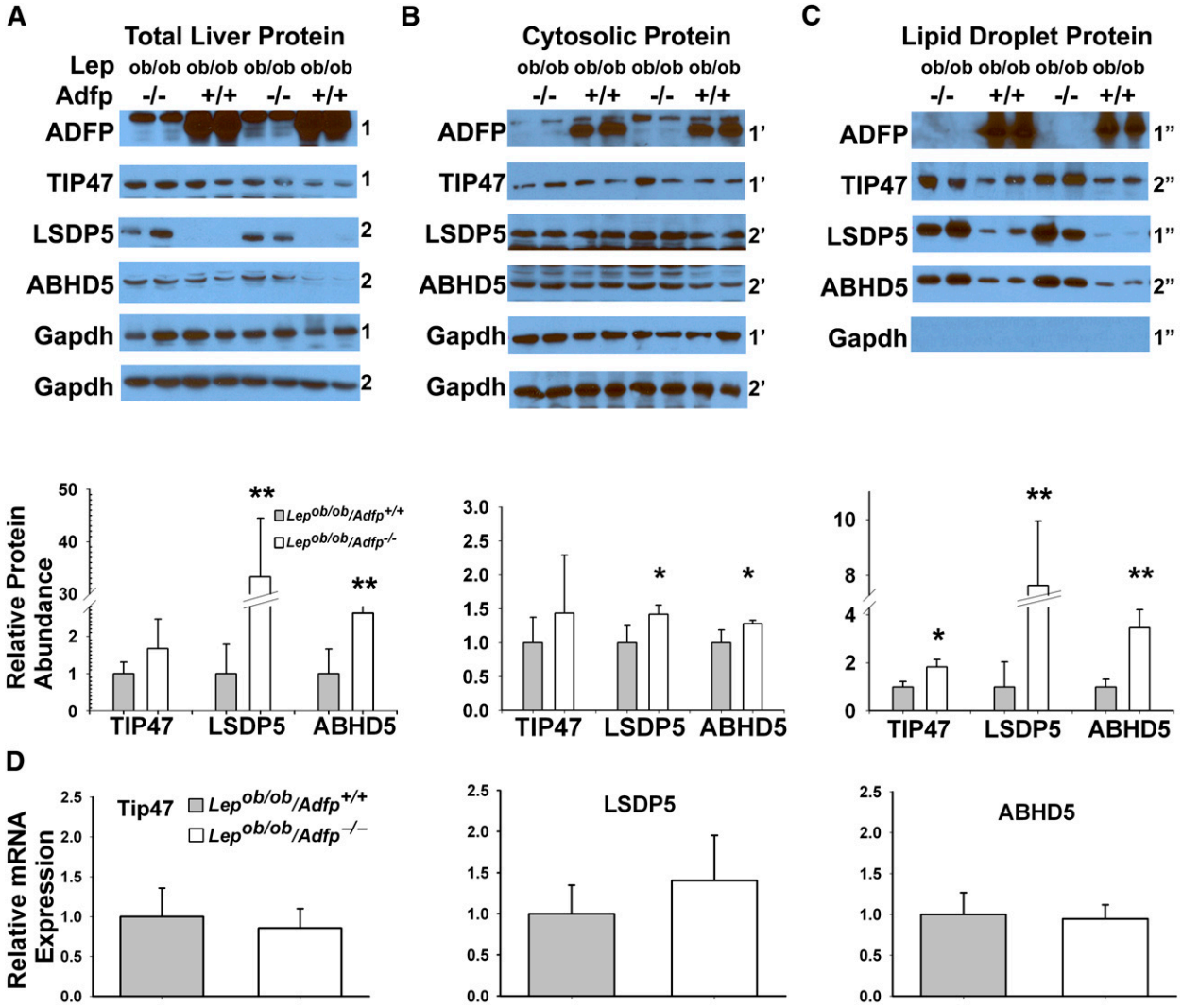

Fig. 5. Liver LD associated protein and mRNA expression analysis. Total (A), cytosolic (B), and LD (C) fractions of liver tissues from $Lep^{ob/ob}/Adfp^{+/+}$ and $Lep^{ob/ob}/Adfp^{-/-}$ mice were isolated as detailed in "Materials and Methods," and Western blot analysis was performed. Because several proteins have very similar molecular weights, multiple protein gels were used. The numbers denoted on the right side of each gel image indicates the gel IDs. A lighter band immediately above the ADFP band in A and B represents cross-reacting material unrelated to ADFP. The very faint ADFP bands in the A and B blots from $Lep^{ob/ob}/Adfp^{-/-}$ mice were the result of slight spill-over from the neighboring $Lep^{ob/ob}/Adfp^{+/+}$ sample wells. Rabbit anti- full-length ADFP and TIP47 proteins (Strategic Diagnostics) were used in these Western blot analyses. Other antibodies were as specified in "Materials and Methods." GAPDH proteins are used as loading control to estimate (using Image J software) the relative protein abundance, shown at the bottom of each panel, between $Lep^{ob/ob}/Adfp^{-/-}$ and $Lep^{ob/ob}/Adfp^{+/+}$ mice. $^{*}P < 0.05$; $^{**}P < 0.01$. GAPDH is not detectable in the Western blot of proteins isolated from LD fraction. Relative protein abundance in LD fraction was therefore estimated using blots that were produced from the identical amount of tissue sample without a non-LDP control (as they were not present in these blots). D: Quantitative RT-PCR analysis of relative Tip47, Lsdp5, and Abhd5 mRNA abundance from $Lep^{ob/ob}/Adfp^{+/+}$ and $Lep^{ob/ob}/Adfp^{-/-}$ liver.

vivo (16) and is not associated with changes in macrophage pro-inflammatory cytokine gene expression (17). In this study, the level of liver enzymes (AST and ALT) was not different in $Lep^{ob/ob}/Adfp^{-/-}$ and $Lep^{ob/ob}/Adfp^{+/+}$ mice. It is interesting that reduced hepatic TG content of the $Lep^{ob/ob}/Adfp^{-/-}$ mice per se, without apparent changes in liver enzymes, appears to be associated with improved glucose intolerance and insulin sensitivity in $Lep^{ob/ob}/Adfp^{-/-}$ mice compared with the $Lep^{ob/ob}/Adfp^{+/+}$ mice. However, in addition to the quantitative change in TG, there were changes in abundance and distribution involving some of the PAT proteins when ADFP was absent. It is unclear if such changes contribute to the improvement of glucose intolerance and insulin sensitivity. Interestingly, hyperinsulinemic-euglycemic clamps indicate that skeletal muscle also exhibits increased glucose uptake in $Lep^{ob/ob}/Adfp^{-/-}$ compared with $Lep^{ob/ob}/Adfp^{+/+}$ mice. Although muscle TG levels are the same between these two groups of mice (data not shown), the muscular tissues are totally surrounded by fat in the obese mice, which may affect the accuracy of TG quantification.

We have previously examined the effect of *Adfp* ablation on LD size and distribution in the liver of C57BL/6 mice following high fat diet-induced hepatosteatosis (16). We found that the total number of LDs identifiable by light microscopy was significantly reduced in $Adfp^{-/-}$ compared

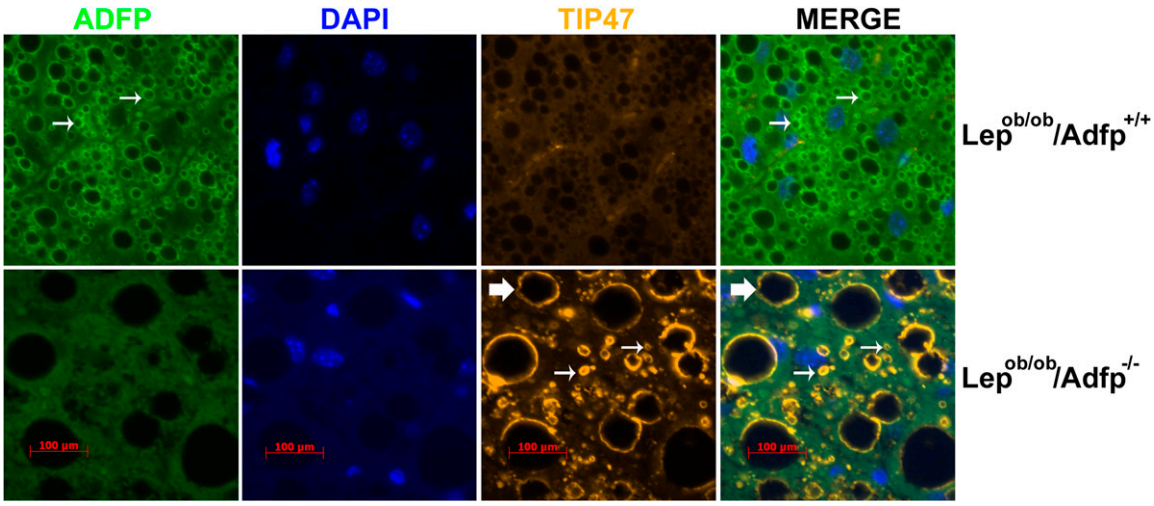

Fig. 6. Immunofluorescence staining of representative liver sections from *Lep*$^{ob/ob}$/*Adfp*$^{+/+}$ and *Lep*$^{ob/ob}$/*Adfp*$^{-/-}$ mice. Guinea pig anti-synthetic human and murine ADFP peptide (N-terminus 1-29 amino acid; Progen GP40) and rabbit anti-mouse TIP47 full-length protein (Strategic Diagnostics) were used in this experiment.

with *Adfp*$^{+/+}$ mouse liver sections (3,247.3 ± 1,228.2 vs. 8,472.8 ± 2,157.6/mm^2) (16). Furthermore, there was a shift in the LD size distribution and "large" LDs became evident in *Adfp*$^{+/+}$ mice that were not found in *Adfp*$^{-/-}$ mice. Superficially, this finding seems to contradict the observation of huge uni- or oligo-locular LDs only in *Lep*$^{ob/ob}$/*Adfp*$^{-/-}$ mice but not in *Lep*$^{ob/ob}$/*Adfp*$^{+/+}$ mice. However, a close examination of the histopathology indicates no real contradiction as we compare the effect of ADFP expression on LD formation in mice with wild-type or *Lep*$^{ob/ob}$ background.

Histological examination of liver sections of lean C57BL/6J mice fed a high-fat diet and *Lep*$^{ob/ob}$ mice (*Lep*$^{ob/ob}$/*Adfp*$^{+/+}$ and *Lep*$^{ob/ob}$/*Adfp*$^{-/-}$ mice) fed regular chow revealed that the fatty change in the liver of mice was much more extreme in mice with *Lep*$^{ob/ob}$ background. The "large" LDs found in ~10% of the hepatocytes in high-fat diet-fed lean *Adfp*$^{+/+}$ mice (but absent in *Adfp*$^{-/-}$ mice) measured up to 15–17 μm in diameter [supplementary Fig. V; also see Fig. 9A in Chang et al. (16)]. On the other hand, 100% of the hepatocytes of *Lep*$^{ob/ob}$ mice were tightly packed with LDs, with the largest droplets measuring up to about 15 μm in diameter. In contrast, ~50% of the hepatocytes in *Lep*$^{ob/ob}$/*Adfp*$^{-/-}$ mice contained giant-sized unilocular or oligolocular LDs that vary greatly in size, with the largest droplets measuring up to 50–90 μm in diameter. In other words, the largest LDs in the liver of *Lep*$^{ob/ob}$/*Adfp*$^{-/-}$ mice hold >100-fold more lipid (by volume) than the largest LDs in the high-fat diet-fed *Adfp*$^{+/+}$ mice (supplementary Fig. V). Thus, absence of ADFP precludes the formation of LDs of moderate sizes (up to 15–17 μm in about 10% of the hepatocytes) in lean C57BL/6J mice with diet-induced fatty liver, whereas the extreme fatty liver of *Lep*$^{ob/ob}$/*Adfp*$^{-/-}$ mice (also in C57BL/6J genetic background) is associated with a reduced number of LDs (that are much smaller than those in *Lep*$^{ob/ob}$/*Adfp*$^{+/+}$ mice) in many hepatocytes. However, the absence of ADFP in this model also leads to the appearance of giant LDs in some other hepatocytes (Fig. 1B; supplementary Fig. V). Although it is tempting to postulate the coalescence of LDs, which has been observed in *Drosophila* S2 cells (41), as the origin of these huge droplets, with ADFP playing an inhibitory role in their formation, we have no direct evidence for this process happening. Importantly, in both lean and *Lep*$^{ob/ob}$ mice, lack of ADFP lowers total hepatic TG content by ~25–60%.

ADFP is the first LDP that appears during adipocyte differentiation in vitro (42). Interestingly, the expression of *Tip47*, *Lsdp5*, and *Abhd5* transcripts in the liver of *Lep*$^{ob/ob}$/*Adfp*$^{-/-}$ mice was not different from that in *Lep*$^{ob/ob}$/*Adfp*$^{+/+}$ mice. The two types of mice also expressed similar amounts of TIP47 at the protein level. TIP47 protein was also unaltered in the absence of ADFP in the retinal pigmented epithelium (19). The concentration of LSDP5 and ABHD5 proteins was, however, increased in the liver of the *Lep*$^{ob/ob}$/*Adfp*$^{-/-}$ mice. It has been shown that ADFP and PERILIPIN are both regulated at the posttranslational levels via degradation through the ubiquitin-mediated proteasome pathway (43, 44). It appears likely that LSDP5 and ABHD5 are also regulated posttranscriptionally in response to changes in the protein composition of LDs or to lipid abundance.

TIP47 is normally distributed mainly in the cytoplasm and is redistributed to LDs when intracellular lipids become abundant (35, 45). In this study, we showed that TIP47 redistributed to the LD surface in the liver when ADFP was absent. This redistribution of TIP47 was evident in Western blots of subcellular fractions as well as in immunofluorescence microscopy (Figs. 5 and 6). The situation appears analogous to THP-1 macrophages in which TIP47 relocated from the cytoplasmic compartment to the surface of LDs when ADFP protein expression was knocked down (46).

TG secretion was reduced in rat hepatoma cells when ABHD5 was knocked down by short hairpin RNA (47), and lipolysis of cytosolic stored TG was part of this process. We showed that ABHD5 is enriched in the LDs of *Lep*$^{ob/ob}$/*Adfp*$^{-/-}$ hepatocytes, and this is accompanied by an increase of VLDL secretion in vivo. However, we did not ob-

serve a change in liver lipase activity (supplementary Fig. VI), although TG hydrolysis assay was done using the liver homogenate that may not reflect the in vivo TG turnover rate. TG synthesis was not altered in primary hepatocytes isolated from $Lep^{ob/ob}/Adfp^{-/-}$ mice compared with that from $Lep^{ob/ob}/Adfp^{+/+}$ hepatocytes (supplementary Fig. VII). In addition, we also did not observe any significant change in gene expression of key enzymes involved in lipid metabolisms (supplementary Fig. II). The detailed molecular interaction between ABHD5, ADFP, and other LDPs in hepatic TG homeostasis remains to be determined.

In conclusion, we created $Lep^{ob/ob}/Adfp^{-/-}$ mice to investigate the role of ADFP and other LDPs in hepatic TG dynamics and whole body glucose homeostasis. We showed that ADFP plays a key role in modulating LD formation and size distribution. In the absence of ADFP, several other LDPs are upregulated in LDs in the liver (Figs. 5C and 6). The presence in a fraction of the $Lep^{ob/ob}/Adfp^{-/-}$ hepatocytes of large uni- and oligo-locular LDs in the absence of ADFP, despite the relocation of other LDPs to the LD, indicates a nonredundant role for ADFP in determining the size of hepatic LDs via mechanisms yet to be determined. The effect of ADFP expression on LD size distribution is complex, and the phenotypic consequence appears to depend in part on the severity of the fatty liver. We further showed that in mice of both wild-type C57BL/6J and $Lep^{ob/ob}$ background, ADFP regulates VLDL secretion in vivo. Moreover, the improvement in fatty liver in the absence of ADFP attenuates the insulin resistance associated with $Lep^{ob/ob}$ mice, both in the liver and in skeletal muscle, underscoring the importance of the degree of fatty liver in regulating whole body glucose homeostasis.

The authors thank Dr. Takashi Osumi of University of Hyogo, Japan, and Dr. Jim McManaman of University of Colorado for a gift of anti-ABHD5 antibody and C-terminal specific anti-ADFP antibody, respectively.

REFERENCES

1. Browning, J. D., L. S. Szczepaniak, R. Dobbins, P. Nuremberg, J. D. Horton, J. C. Cohen, S. M. Grundy, and H. H. Hobbs. 2004. Prevalence of hepatic steatosis in an urban population in the United States: impact of ethnicity. *Hepatology.* **40:** 1387–1395.
2. Murphy, D. J., I. Hernendez-Pinzon, K. Patel, R. G. Hope, and J. McLauchlan. 2000. New insights into the mechanisms of lipid-body biogenesis in plants and other organisms. *Biochem. Soc. Trans.* **28:** 710–711.
3. Londos, C., C. Sztalryd, J. T. Tansey, and A. R. Kimmel. 2005. Role of PAT proteins in lipid metabolism. *Biochimie.* **87:** 45–49.
4. Londos, C., D. L. Brasaemle, C. J. Schultz, D. C. dler-Wailes, D. M. Levin, A. R. Kimmel, and C. M. Rondinone. 1999. On the control of lipolysis in adipocytes. *Ann. N. Y. Acad. Sci.* **892:** 155–168.
5. Miura, S., J. W. Gan, J. Brzostowski, M. J. Parisi, C. J. Schultz, C. Londos, B. Oliver, and A. R. Kimmel. 2002. Functional conservation for lipid storage droplet association among Perilipin, ADRP, and TIP47 (PAT)-related proteins in mammals, Drosophila, and Dictyostelium. *J. Biol. Chem.* **277:** 32253–32257.
6. Liu, P., Y. Ying, Y. Zhao, D. I. Mundy, M. Zhu, and R. G. Anderson. 2004. Chinese hamster ovary K2 cell lipid droplets appear to be metabolic organelles involved in membrane traffic. *J. Biol. Chem.* **279:** 3787–3792.
7. Brasaemle, D. L., G. Dolios, L. Shapiro, and R. Wang. 2004. Proteomic analysis of proteins associated with lipid droplets of basal and lipolytically stimulated 3T3–L1 adipocytes. *J. Biol. Chem.* **279:** 46835–46842.
8. Sato, S., M. Fukasawa, Y. Yamakawa, T. Natsume, T. Suzuki, I. Shoji, H. Aizaki, T. Miyamura, and M. Nishijima. 2006. Proteomic profiling of lipid droplet proteins in hepatoma cell lines expressing hepatitis C virus core protein. *J. Biochem.* **139:** 921–930.
9. Chang, B. H., and L. Chan. 2007. Regulation of triglyceride metabolism. III. Emerging role of lipid droplet protein ADFP in health and disease. *Am. J. Physiol. Gastrointest. Liver Physiol.* **292:** G1465–G1468.
10. Brasaemle, D. L. 2007. Thematic review series: adipocyte biology. The perilipin family of structural lipid droplet proteins: stabilization of lipid droplets and control of lipolysis. *J. Lipid Res.* **48:** 2547–2559.
11. Wolins, N. E., D. L. Brasaemle, and P. E. Bickel. 2006. A proposed model of fat packaging by exchangeable lipid droplet proteins. *FEBS Lett.* **580:** 5484–5491.
12. Ducharme, N. A., and P. E. Bickel. 2008. Lipid droplets in lipogenesis and lipolysis. *Endocrinology.* **149:** 942–949.
13. Kimmel, A. R., D. L. Brasaemle, M. McAndrews-Hill, C. Sztalryd, and C. Londos. 2010. Adoption of PERILIPIN as a unifying nomenclature for the mammalian PAT-family of intracellular lipid storage droplet proteins. *J. Lipid Res.* **51:** 468–471.
14. Martinez-Botas, J., J. B. Anderson, D. Tessier, A. Lapillonne, B. H. Chang, M. J. Quast, D. Gorenstein, K. H. Chen, and L. Chan. 2000. Absence of perilipin results in leanness and reverses obesity in Lepr(db/db) mice. *Nat. Genet.* **26:** 474–479.
15. Tansey, J. T., C. Sztalryd, J. Gruia-Gray, D. L. Roush, J. V. Zee, O. Gavrilova, M. L. Reitman, C. X. Deng, C. Li, A. R. Kimmel, et al. 2001. Perilipin ablation results in a lean mouse with aberrant adipocyte lipolysis, enhanced leptin production, and resistance to diet-induced obesity. *Proc. Natl. Acad. Sci. USA.* **98:** 6494–6499.
16. Chang, B. H., L. Li, A. Paul, S. Taniguchi, V. Nannegari, W. C. Heird, and L. Chan. 2006. Protection against fatty liver but normal adipogenesis in mice lacking adipose differentiation-related protein. *Mol. Cell. Biol.* **26:** 1063–1076.
17. Paul, A., B. H. Chang, L. Li, V. K. Yechoor, and L. Chan. 2008. Deficiency of adipose differentiation-related protein impairs foam cell formation and protects against atherosclerosis. *Circ. Res.* **102:** 1492–1501.
18. Russell, T. D., C. A. Palmer, D. J. Orlicky, E. S. Bales, B. H. Chang, L. Chan, and J. L. McManaman. 2008. Mammary glands of adipophilin-null mice produce an amino-terminally truncated form of adipophilin that mediates milk lipid droplet formation and secretion. *J. Lipid Res.* **49:** 206–216.
19. Imanishi, Y., W. Sun, T. Maeda, A. Maeda, and K. Palczewski. 2008. Retinyl ester homeostasis in the adipose differentiation-related protein deficient retina. *J. Biol. Chem.* **283:** 25091–25102.
20. Wolins, N. E., J. R. Skinner, M. J. Schoenfish, A. Tzekov, K. G. Bensch, and P. E. Bickel. 2003. Adipocyte protein S3–12 coats nascent lipid droplets. *J. Biol. Chem.* **278:** 37713–37721.
21. Yamaguchi, T., S. Matsushita, K. Motojima, F. Hirose, and T. Osumi. 2006. MLDP, a novel PAT family protein localized to lipid droplets and enriched in the heart, is regulated by peroxisome proliferator-activated receptor alpha. *J. Biol. Chem.* **281:** 14232–14240.
22. Wolins, N. E., B. K. Quaynor, J. R. Skinner, A. Tzekov, M. A. Croce, M. C. Gropler, V. Varma, A. Yao-Borengasser, N. Rasouli, P. A. Kern, et al. 2006. OXPAT/PAT-1 is a PPAR-induced lipid droplet protein that promotes fatty acid utilization. *Diabetes.* **55:** 3418–3428.
23. Chehab, F. F., J. Qiu, and S. Ogus. 2004. The use of animal models to dissect the biology of leptin. *Recent Prog. Horm. Res.* **59:** 245–266.
24. Monetti, M., M. C. Levin, M. J. Watt, M. P. Sajan, S. Marmor, B. K. Hubbard, R. D. Stevens, J. R. Bain, C. B. Newgard, R. V. Farese, Sr., et al. 2007. Dissociation of hepatic steatosis and insulin resistance in mice overexpressing DGAT in the liver. *Cell Metab.* **6:** 69–78.
25. Ginsberg, H. N., Y. L. Zhang, and A. Hernandez-Ono. 2005. Regulation of plasma triglycerides in insulin resistance and diabetes. *Arch. Med. Res.* **36:** 232–240.
26. Chang, B. H., W. Liao, L. Li, M. Nakamuta, D. Mack, and L. Chan. 1999. Liver-specific inactivation of the abetalipoproteinemia gene completely abrogates very low density lipoprotein/low density lipoprotein production in a viable conditional knockout mouse. *J. Biol. Chem.* **274:** 6051–6055.
27. Bligh, E. G., and W. J. Dyer. 1959. A rapid method of total lipid extraction and purification. *Can. J. Biochem. Physiol.* **37:** 911–917.

28. Schwartz, D. M., and N. E. Wolins. 2007. A simple and rapid method to assay triacylglycerol in cells and tissues. *J. Lipid Res.* **48:** 2514–2520.
29. Millar, J. S., D. A. Cromley, M. G. McCoy, D. J. Rader, and J. T. Billheimer. 2005. Determining hepatic triglyceride production in mice: comparison of poloxamer 407 with Triton WR-1339. *J. Lipid Res.* **46:** 2023–2028.
30. Vandesompele, J., P. K. De, F. Pattyn, B. Poppe, R. N. Van, P. A. De, and F. Speleman. 2002. Accurate normalization of real-time quantitative RT-PCR data by geometric averaging of multiple internal control genes. *Genome Biol.* **3**: RESEARCH0034.
31. Matsumura, K., B. H. Chang, M. Fujimiya, W. Chen, R. N. Kulkarni, Y. Eguchi, H. Kimura, H. Kojima, and L. Chan. 2007. Aquaporin 7 is a beta-cell protein and regulator of intraislet glycerol content and glycerol kinase activity, beta-cell mass, and insulin production and secretion. *Mol. Cell. Biol.* **27:** 6026–6037.
32. Saha, P. K., H. Kojima, J. Martinez-Botas, A. L. Sunehag, and L. Chan. 2004. Metabolic adaptations in the absence of perilipin: increased beta-oxidation and decreased hepatic glucose production associated with peripheral insulin resistance but normal glucose tolerance in perilipin-null mice. *J. Biol. Chem.* **279:** 35150–35158.
33. Cox, B., and A. Emili. 2006. Tissue subcellular fractionation and protein extraction for use in mass-spectrometry-based proteomics. *Nat. Protoc.* **1:** 1872–1878.
34. Liu, P., R. Bartz, J. K. Zehmer, Y. Ying, and R. G. Anderson. 2008. Rab-regulated membrane traffic between adiposomes and multiple endomembrane systems. *Methods Enzymol.* **439:** 327–337.
35. Sztalryd, C., M. Bell, X. Lu, P. Mertz, S. Hickenbottom, B. H. Chang, L. Chan, A. R. Kimmel, and C. Londos. 2006. Functional compensation for adipose differentiation-related protein (ADFP) by Tip47 in an ADFP null embryonic cell line. *J. Biol. Chem.* **281:** 34341–34348.
36. Orlicky, D. J., G. Degala, C. Greenwood, E. S. Bales, T. D. Russell, and J. L. McManaman. 2008. Multiple functions encoded by the N-terminal PAT domain of adipophilin. *J. Cell Sci.* **121:** 2921–2929.
37. Imai, Y., G. M. Varela, M. B. Jackson, M. J. Graham, R. M. Crooke, and R. S. Ahima. 2007. Reduction of hepatosteatosis and lipid levels by an adipose differentiation-related protein antisense oligonucleotide. *Gastroenterology.* **132:** 1947–1954.
38. Chitturi, S., and G. C. Farrell. 2007. Fatty liver now, diabetes and heart attack later? The liver as a barometer of metabolic health. *J. Gastroenterol. Hepatol.* **22:** 967–969.
39. Carpentier, A., C. Taghibiglou, N. Leung, L. Szeto, S. C. Van Iderstine, K. D. Uffelman, R. Buckingham, K. Adeli, and G. F. Lewis. 2002. Ameliorated hepatic insulin resistance is associated with normalization of microsomal triglyceride transfer protein expression and reduction in very low density lipoprotein assembly and secretion in the fructose-fed hamster. *J. Biol. Chem.* **277:** 28795–28802.
40. Tilg, H., and A. R. Moschen. 2008. Insulin resistance, inflammation, and non-alcoholic fatty liver disease. *Trends Endocrinol. Metab.* **19:** 371–379.
41. Guo, Y., T. C. Walther, M. Rao, N. Stuurman, G. Goshima, K. Terayama, J. S. Wong, R. D. Vale, P. Walter, and R. V. Farese. 2008. Functional genomic screen reveals genes involved in lipid-droplet formation and utilization. *Nature.* **453:** 657–661.
42. Brasaemle, D. L., T. Barber, N. E. Wolins, G. Serrero, E. J. Blanchette-Mackie, and C. Londos. 1997. Adipose differentiation-related protein is an ubiquitously expressed lipid storage droplet-associated protein. *J. Lipid Res.* **38:** 2249–2263.
43. Xu, G., C. Sztalryd, X. Lu, J. T. Tansey, J. Gan, H. Dorward, A. R. Kimmel, and C. Londos. 2005. Post-translational regulation of adipose differentiation-related protein by the ubiquitin/proteasome pathway. *J. Biol. Chem.* **280:** 42841–42847.
44. Xu, G., C. Sztalryd, and C. Londos. 2006. Degradation of perilipin is mediated through ubiquitination-proteasome pathway. *Biochim. Biophys. Acta.* **1761:** 83–90.
45. Zhu, J., B. Lee, K. K. Buhman, and J. X. Cheng. 2009. A dynamic, cytoplasmic triacylglycerol pool in enterocytes revealed by ex vivo and in vivo coherent anti-Stokes Raman scattering imaging. *J. Lipid Res.* **50:** 1080–1089.
46. Buers, I., H. Robenek, S. Lorkowski, Y. Nitschke, N. J. Severs, and O. Hofnagel. 2009. TIP47, a lipid cargo protein involved in macrophage triglyceride metabolism. *Arterioscler. Thromb. Vasc. Biol.* **29:** 767–73.
47. Caviglia, J. M., J. D. Sparks, N. Toraskar, A. M. Brinker, T. C. Yin, J. L. Dixon, and D. L. Brasaemle. 2009. ABHD5/CGI-58 facilitates the assembly and secretion of apolipoprotein B lipoproteins by McA RH7777 rat hepatoma cells. *Biochim. Biophys. Acta.* **1791:** 198–205.